TOWARDS STUDIES OF RARE DECAYS OF POSITRONIUM WITH J-PET*

Pooja Tanty, Elena Perez del Rio, Pawel Moskal

on behalf of the J-PET Collaboration

Faculty of Physics, Astronomy, and Applied Computer Science
Jagiellonian University, 30-348 Kraków, Poland
and
Centre for Theranostics, Jagiellonian University, 31-501 Kraków, Poland

Received 8 February 2024, accepted 13 February 2024, published online 26 February 2024

The positronium system, a bound state of an electron and a positron, is suitable for testing the predictions of quantum electrodynamics (QED) as well as symmetry invariance. The Ps triple state, the ortho-Positronium (o-Ps), which mainly decays to three photons, is further studied to search for decays into 4γ and 5γ, the former C-violating decay and the latter never observed. The J-PET is a multi-purpose detector optimized for the detection of photons from positron–electron annihilation and can be used in a broad scope of interdisciplinary investigation. The large acceptance and high angular resolution of the J-PET detector will push the present limits in these forbidden and rare decays. The aim is to reach a sensitivity below $O(10^{-6})$ while reducing the uncertainties, thus increasing the sensitivity.

DOI:10.5506/APhysPolBSupp.17.1-A9

1. Introduction

The positronium being a bound state of an electron and positron is well understood by the Quantum Electrodynamics (QED) [1, 2]. In the ground state, it is available in two configurations, the singlet state para-positronium (p-Ps) and the triplet state ortho-positronium (o-Ps) with lifetimes of 125 ps and 142 ns, respectively. Since the o-Ps decays are dominated by the electromagnetic interactions, which conserve the charge conjugation parity, the o-Ps is allowed to decay into an odd number of gamma quanta: o-Ps $\rightarrow 3\gamma, 5\gamma, 7\gamma$, and so on. Being a purely leptonic system, positronium is an effective testing ground for QED and precision studies in the absence of any hadronic background contribution.

* Presented at the Symposium on *New Trends in Nuclear and Medical Physics*, Kraków, Poland, 18–20 October, 2023.

1.1. Rare and forbidden decays of o-Ps

Ortho-positronium predominantly decays into three gamma quanta, while the rate for a higher number of photons is by six orders of magnitude smaller than expected from QED calculations [3]. Measurements of five photon decay are consistent with both zero and theoretical expectations. Previous bounds were obtained on branching ratio by Matsumoto *et al.* [4] $\mathrm{BR}(\text{o-Ps} \to 5\gamma) = [2.2^{+2.6}_{-1.6} \pm 0.5] \times 10^{-6}$, and Vetter and Freedman [5] $\mathrm{BR}(\text{o-Ps} \to 5\gamma) = [1.67 \pm 0.99 \pm 0.37] \times 10^{-6}$. The tree-level theoretical calculation of the branching ratio for this rare decay mode o-Ps $\to 5\gamma$ has been reported in previous works [3, 6]. The resulting branching ratio is given by $\mathrm{BR}(\text{o-Ps} \to 5\gamma) = [0.9591(8)] \times 10^{-6}$, as documented in Ref. [7]. The $\mathrm{BR}(\text{o-Ps} \to 5\gamma)$ is determined experimentally by several orders of magnitude less precise than it is estimated theoretically. This motivates us for more precise measurements of BR for this rare decay channel.

Positronium is an eigenstate of charge conjugation operator, C, which forces o-Ps to decay into an odd number of photons [8, 9]. Ortho-positronium decaying into 4 gammas is forbidden by the charge conjugation invariance. The branching ratio for these decays (Standard Model (SM) calculation) is of the order of 10^{-10}–10^{-9} [10]. Observation of a branching ratio greater than predicted by the SM would suggest a violation of C symmetry [11, 12]. The present limits on this decay mode is found to be: $\mathrm{BR}(\text{o-Ps} \to 4\gamma/\text{o-Ps} \to 3\gamma) < 2.6 \times 10^{-6}$ at 90% C.L. [13].

To search for these rare and forbidden multi-photon decays, the potential of the Jagiellonian Positron Emission Tomograph has been utilized [14–19].

2. Jagiellonian Positron Emission Tomograph (J-PET)

The present study has been done with the multipurpose Jagiellonian Positron Emission Tomography scanner built for research in the field of fundamental physics [14] and medical diagnostics [19–21]. It is made up of 192, EJ-230 plastic scintillator strips of dimensions $50 \times 1.9 \times 0.7$ cm^3. These scintillator strips are arranged in 3 layers of concentric cylinders with diameters 42.5 cm, 46.75 cm, and 57.5 cm along the longitudinal axis of the scanner (Fig. 1) [22, 23]. The ends of the scintillators are coupled with the Hamamatsu R9800 vacuum tube photomultiplier tubes (PMTs). Gamma quanta from Ps annihilation interact with the plastic scintillator via the Compton scattering resulting in the emission of scintillation light detected in both the PMTs. The electrical signals from the PMTs are sampled at four voltage thresholds at the leading and trailing edges with dedicated digital front-end electronics [24]. This cost-effective scanner has a large field of view (50 cm) and triggerless data acquisition [25] allowing for the detection of multi-photon decays.

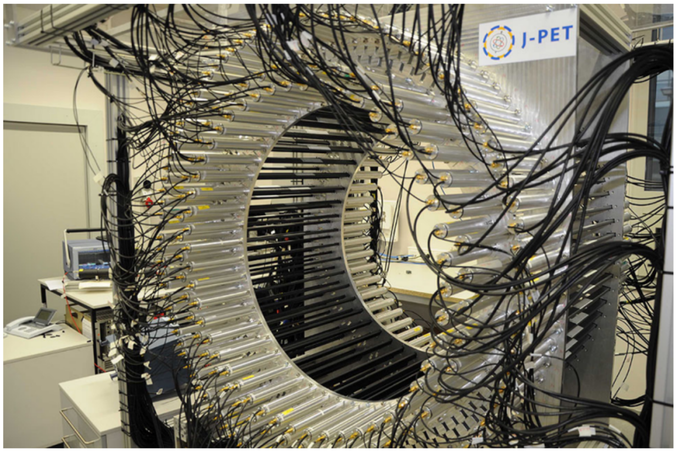

Fig. 1. Image of the first prototype of Jagiellonian Positron Emission Tomograph.

A radioactive isotope was used as a positron source. This measurement was performed with Na-22 in a small plastic chamber. The inside of the plastic chamber [26] is coated with porous material XAD4 to enhance the production of o-Ps to 29% [27]. In 90% of the cases, Na-22 undergoes β^+ decay. During the beta decay of Na-22, a positron is emitted with an excited neon atom. The excited neon de-excites to its ground state emitting gamma quanta of 1274 keV energy. The decayed positron thermalizes in the porous material and forms positronium [1]. The presence of XAD4 facilitates the production of o-Ps. The emission of this de-excitation gamma occurs on average in about 1.6 ps after the emission of the positron [28], therefore, the time of its emission may be considered as the time of the formation of o-Ps. Hence the signal from de-excited gamma can be used as the start signal for the o-Ps lifetime calculation [1, 17].

As mentioned above, the signals from the interaction of gamma quanta in plastic scintillators are extracted through the PMTs. These signals are further sampled at four voltage thresholds. The times extracted from both sides of the PMTs are used to determine the place of gamma quanta interaction. Also, the annihilation point is determined using the time-of-flight (TOF) method. The data acquisition from the detector is in triggerless mode [24, 25] allowing us to use the same data for different studies. The stored data is further analyzed via a dedicated framework developed for J-PET analysis [29].

3. Results and discussions

The primary aim is to determine the branching ratio of the above-mentioned decay channels.

3.1. Preliminary data analysis

For this study, the data collected during Run 11 of the J-PET prototype was used. Commencing on April 2, 2020, and concluding on March 1, 2021, the aforementioned run lasted almost for a year. The data collection includes 250 days of measurement with Na-22 source and 60 days of data with the cosmic background. In the analysis, Time Over Threshold (TOT) is used as an estimate of energy deposition of gamma quanta in the plastic scintillator [30]. Events are categorized as annihilation or de-excitation based on the TOT values of the hits. A preliminary counting of the events is based on the number of photons registered in the event. A total of 10,000 files of data have been used for the analysis. The estimated number of events for the complete Run 11 has been given in Fig. 2 as a function of hits multiplicity in the event.

Annihilation including prompt

Hits Multiplicity	Estimated counts
3	1.54×10^8
4	1.38×10^7
5	8.05×10^5
6	3.6×10^4
7	1.04×10^3

$$\text{Counts X } \frac{total\ number\ of\ files}{total\ files\ analyzed}$$

Only annihilation

Hits Multiplicity	Estimated counts
2	7.3×10^8
3	5.97×10^8
4	3.2×10^7
5	1.3×10^6
6	5.3×10^4
7	1.7×10^3

Fig. 2. Estimation of the number of collected events as a function of multiplicity of hits in the event.

3.2. Toy Monte Carlo for efficiency estimation

The calculation of the branching ratio of multi-photon decays of o-Ps requires the gamma quanta detection efficiency of J-PET [31]. In this work, for preliminary estimation, this detection efficiency has been calculated with a dedicated toy Monte Carlo model as the product of the single efficiencies due to the registration efficiency, the detection efficiency and the geometrical efficiency. For the efficiency calculation, events are generated in pure phase space using ROOT TGenPhaseSpace [32] event generator. Here is a brief description of the different efficiencies included in the toy MC model:

— Geometrical efficiency (ϵ_{geo}) — It assumes the detector to be a solid cylinder for a simplified case; The solid angle subtended by a cylinder when viewed by a point inside is here naively considered as the acceptance of the detector. After generating events in pure phase space, the events are checked to be within the detector acceptance range. The detector acceptance includes θ ranging from 60 to 120 degrees and ϕ from $-\pi$ to π. The ratio of multi-photon events detected within the detector acceptance (N_{geo}) to the total number of events generated in phase space (N_{gen}) is the geometrical efficiency

$$\epsilon_{\text{geo}} = \frac{N_{\text{geo}}}{N_{\text{gen}}} \,. \tag{1}$$

— Detection efficiency (ϵ_{det}) — It encompasses the transmission probability of photons through the plastic scintillator of the thickness (x) of 2 cm. The mass attenuation coefficient (μ) of plastic is energy-dependent. The values of mass attenuation coefficient for different energy values were taken from the NIST database [33]. Furthermore, the mass attenuation coefficients were interpolated for the different incoming energies of the photons which are within the detector acceptance (N_{geo}). The probability of photons interacting in the plastic scintillator is given by

$$P = 1 - \mathrm{e}^{-\mu x} \,. \tag{2}$$

For each photon in an event, the probability of it interacting with the scintillator material is calculated. The events are further sampled taking into account the product of the interaction probability of all the photons in an event using the rejection sampling. The ratio of the number of events surviving rejection sampling (N_{det}) to the total number of events in the geometrical acceptance (N_{geo}) is considered the detection efficiency

$$\epsilon_{\text{det}} = \frac{N_{\text{det}}}{N_{\text{geo}}} \,. \tag{3}$$

— Registration efficiency (ϵ_{reg}) — This parameter takes care of the scattering of photons in the plastic scintillator. The energy of the Compton scattered recoil electrons is a measure of deposited energy of kinematically allowed multi-photon events. For this study, events with 4 or 5 photons have been considered. The differential cross section for the photon interaction is calculated using the Klein–Nishina formula

$$\frac{\mathrm{d}\sigma}{\mathrm{d}\Omega} = \frac{r_0^2}{2}\left(\frac{E'}{E}\right)^2\left[\frac{E}{E'} + \frac{E'}{E} - \sin^2(\theta)\right] , \tag{4}$$

where r_0 is electron radius, E/E' is the ratio of energies of the incident and scattered photons, and θ is the scattering angle of the photon.

However, $\frac{\mathrm{d}\sigma}{\mathrm{d}E_{\mathrm{recoil}}}$ is used to calculate the energy spectrum of the deposited energy.

First, the cross section of the incoming energy of photons interacting with the plastic scintillator is sampled using the rejection sampling technique. Later, the smallest deposited energy of the incoming photon is calculated. To limit the electronic noise from DAQ, a limit of 30 keV is applied. Events having photons of energy above 30 keV are considered for calculation of registration efficiency. The ratio of the number of events in which all photons have deposited energies larger than 30 keV (N_{reg}) to the total number of events interacting with the plastic scintillator (N_{det}) is considered as the registration efficiency

$$\epsilon_{\mathrm{reg}} = \frac{N_{\mathrm{reg}}}{N_{\mathrm{det}}} \,. \tag{5}$$

The total efficiency is calculated as the product of the above three relative efficiencies:

$$\epsilon_{\mathrm{total}} = \frac{N_{\mathrm{geo}}}{N_{\mathrm{gen}}} \frac{N_{\mathrm{det}}}{N_{\mathrm{geo}}} \frac{N_{\mathrm{reg}}}{N_{\mathrm{det}}} \,, \tag{6}$$

$$\epsilon_{\mathrm{total}} = \epsilon_{\mathrm{reg}}\, \epsilon_{\mathrm{det}}\, \epsilon_{\mathrm{geo}} \,. \tag{7}$$

The efficiency obtained from the MC has been summarized in Table 1.

Table 1. Efficiencies obtained from MC. ϵ_{geo} is the geometrical acceptance in a toy version of J-PET, ϵ_{det} is the interaction probability of photons in the plastic scintillator of thickness 2 cm, ϵ_{reg} takes into account the Compton scattering of photons with the scintillator material. $\epsilon_{\mathrm{total}}$ is the total efficiency calculated.

Relative efficiencies (in %)	4γ	5γ
ϵ_{geo}	11.75	5.9
ϵ_{det}	0.34	0.15
ϵ_{reg}	31.8	17.39
Total efficiency (in %)	4γ	5γ
$\epsilon_{\mathrm{total}} : \epsilon_{\mathrm{reg}}\, \epsilon_{\mathrm{det}}\, \epsilon_{\mathrm{geo}}$	0.013	0.0016

Figure 3 shows the simulated smallest deposited energy of the photons with the toy MC after applying the detector resolution. With the events obtained through the preliminary data analysis along with the efficiencies calculated via toy MC, the branching ratio will be estimated.

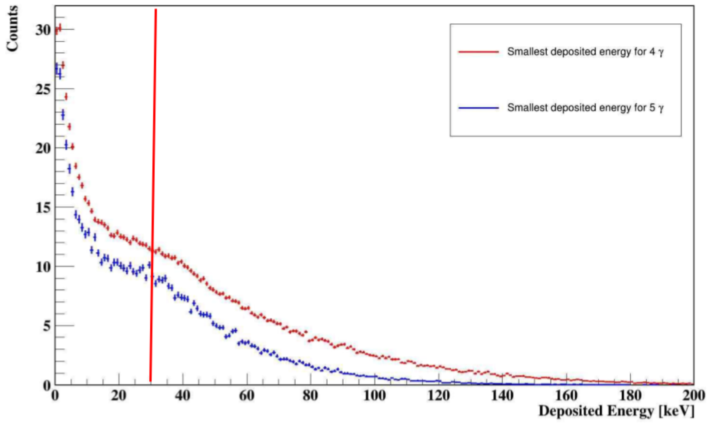

Fig. 3. The smallest energy deposition is shown for 4γ and 5γ events genereated using TGenPhaseSpace. A threshold of 30 keV is applied to limit the electronic noise from the DAQ.

4. Conclusions

In this work, we have presented the preliminary results from the data acquired during Run 11 of the first J-PET prototype. In addition to that, we have simulated a toy Monte Carlo model to estimate the efficiency of J-PET in registering the gamma quanta from the rare and forbidden decays of o-Ps. For proper calculation of the o-PS candidate, more refined and strict selection criteria need to be introduced in the future, like Deep Neural Networks (DNN) to discriminate the decay channels. The idea is to increase the purity while reducing enough the backgrounds to achieve the desired sensitivity of at least $O(10^{-6})$, pushing present limits in these rare and forbidden decays.

We acknowledge support from the National Science Centre (NCN), Poland through grants No. 2019/35/B/ST2/03562, 2020/38/E/ST2/00112, the Ministry of Education and Science through grant No. SPUB/SP/490528/2021, and the SciMat and qLife Priority Research Area budget under the auspices of the program Excellence Initiative-Research University at the Jagiellonian University.

REFERENCES

[1] S.D. Bass *et al.*, *Rev. Mod. Phys.* **95**, 021002 (2023).

[2] S.D. Bass, *Acta Phys. Pol. B* **50**, 1319 (2019).

[3] A. Ore, J.L. Powell, *Phys. Rev.* **75**, 1696 (1949).
[4] T. Matsumoto *et al.*, *Phys. Rev. A* **54**, 1947 (1996).
[5] P.A. Vetter, S.J. Freedman, *Phys. Rev. A* **66**, 052505 (2002).
[6] G.S. Adkins, F.R. Brown, *Phys. Rev. A* **28**, 1164 (1983).
[7] G.P. Lepage *et al.*, *Phys. Rev. A* **28**, 3090 (1983).
[8] S. Berko, H.N. Pendleton, *Annu. Rev. Nucl. Part. Sci.* **30**, 543 (1980).
[9] A. Rich, *Rev. Mod. Phys.* **53**, 127 (1981).
[10] H.S. Mani, A. Rich, *Phys. Rev. D* **4**, 122 (1971).
[11] K. Marko, A. Rich, *Phys. Rev. Lett.* **33**, 980 (1974).
[12] A.P. Mills, S. Berko, *Phys. Rev. Lett.* **18**, 420 (1967).
[13] J. Yang *et al.*, *Phys. Rev. A* **54**, 1952 (1996).
[14] P. Moskal *et al.*, *Acta Phys. Pol. B* **47**, 509 (2016).
[15] P. Moskal *et al.*, *Nat. Commun.* **12**, 5658 (2021).
[16] F. Tayefi Ardebili *et al.*, *Bio-Algorithms Med-Syst.* **19**, 132 (2023).
[17] P. Moskal *et al.*, *Sci. Adv.* **7**, 4394 (2021).
[18] P. Moskal *et al.*, *Nat. Commun.* **15**, 78 (2024).
[19] P. Moskal *et al.*, *PET Clin.* **15**, 439 (2020).
[20] E.Y. Bayene *et al.*, *Bio-Algorithms Med-Syst.* **19**, 101 (2023).
[21] P. Konieczka *et al.*, *Bio-Algorithms Med-Syst.* **19**, 43 (2023).
[22] P. Moskal *et al.*, *Nucl. Instrum. Methods Phys. Res. A* **764**, 317 (2014).
[23] S. Niedźwiecki *et al.*, *Acta Phys. Pol. B* **48**, 1567 (2017).
[24] G. Korcyl *et al.*, *Acta Phys. Pol. B* **47**, 491 (2016).
[25] G. Korcyl *et al.*, *IEEE Trans. Med. Imag.* **37**, 2526 (2018).
[26] M. Gorgol *et al.*, *Acta Phys. Pol. B* **51**, 293 (2020).
[27] B. Jasińska *et al.*, *Acta Phys. Pol. B* **47**, 453 (2016).
[28] M. Das *et al.*, *Bio-Algorithms Med-Syst.* **19**, 87 (2023).
[29] W. Krzemień *et al.*, *Acta Phys. Pol. A* **127**, 1491 (2015).
[30] S. Sharma *et al.*, *EJNMMI Phys.* **7**, 39 (2020).
[31] S. Sharma *et al.*, *EJNMMI Phys.* **10**, 28 (2023).
[32] `https://root.cern.ch/doc/v608/classTGenPhaseSpace.html`
[33] `https://physics.nist.gov/PhysRefData/XrayMassCoef/ComTab/vinyl.html`